

Simple Yet Efficient: Towards Self-Supervised FG-SBIR with Unified Sample Feature Alignment

Jianan Jiang¹, Di Wu¹, Zhilin Jiang¹, Weiren Yu²

¹Hunan University, ²University of Warwick

jiangjn22@hnu.edu.cn, dwu@hnu.edu.cn, zhilin@hnu.edu.cn, Weiren.Yu@warwick.ac.uk

Abstract

Fine-Grained Sketch-Based Image Retrieval (FG-SBIR) aims to minimize the distance between sketches and corresponding images in the embedding space. However, scalability is hindered by the growing complexity of solutions, mainly due to the abstract nature of fine-grained sketches. In this paper, we propose a simple yet efficient approach to narrow the gap between the two modes. It mainly facilitates unified mutual information sharing both intra- and inter-samples, rather than treating them as a single feature alignment problem between modalities. Specifically, our approach includes: (i) Employing dual weight-sharing networks to optimize alignment within sketch and image domain, which also effectively mitigates model learning saturation issues. (ii) Introducing an objective optimization function based on contrastive loss to enhance the model's ability to align features intra- and inter-samples. (iii) Presenting a learnable TRSM combined of self-attention and cross-attention to promote feature representations among tokens, further enhancing sample alignment in the embedding space. Our framework achieves excellent results on CNN- and ViT-based backbones. Extensive experiments demonstrate its superiority over existing methods. We also introduce Cloths-V1, the first professional fashion sketches and images dataset, utilized to validate our method and will be beneficial for other applications.¹

Introduction

With the continuous evolution of artificial intelligence technologies (Xu et al. 2024; Wang et al. 2023; Baldi et al. 2023; Deng et al. 2024; Wu et al. 2023), it has catalyzed disruptive technological transformations in the field of design. Sketch (Xu et al. 2022) serves as a fundamental tool for designers, offering a vital medium for expressing new ideas. Moreover, Sketch-Based Image Retrieval (SBIR) (Wang et al. 2019; Wei et al. 2021; Yu et al. 2021) stands as a fundamental task, it streamlines the process for designers by enabling them to avoid irrelevant images when searching for reference materials. This capability allows designers to swiftly translate abstract concepts into sketches and retrieve closely related images, thereby significantly enhancing productivity and fostering creativity.

Starting with (Yu et al. 2016), the triplet loss has gained prominence in the field of Fine-Grained SBIR. It encourages

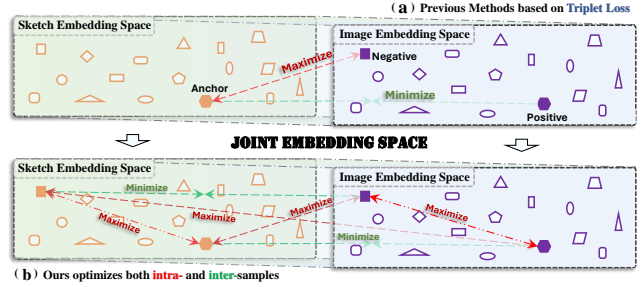


Figure 1: Comparison of sample distribution optimization principles in the joint embedding space, our method simultaneously optimizes both intra- and inter-samples more comprehensively.

proximity among similar samples in the embedding space while pushing different samples farther apart as shown in Fig. 1 (a), thereby achieving effective separation of samples. However, the selection of suitable triplets necessitates further refinement to achieve optimal performance. Moreover, in some cases, the triplet loss might not provide sufficient gradient signals, thereby affecting the model optimization process. To address these challenges, methods like reinforcement learning (Muhammad et al. 2018; Bhunia et al. 2020, 2022a), meta-learning (Sain et al. 2021; Bhunia et al. 2022b), and out-of-sample learning (Sain et al. 2023) have emerged. These approaches aim to refine the model's retrieval capabilities. However, such strategies may introduce instability during model training and pose challenges in tuning hyperparameters. For instance, (Sain et al. 2021) encounters issues of gradient vanishing, while (Bhunia et al. 2021) may exhibit sensitivity to hyperparameters. These challenges collectively compromise the overall model scalability, making it challenging for researchers in the community to further expand their research.

Furthermore, several methods (Sain et al. 2020; Yang et al. 2021; Pang et al. 2020) divide input sketches into strokes or layers, introducing additional complexity within the research community. These might be less compatible with other datasets and less adaptable to broader exploration. In summary, triplet loss has achieved widespread adoption and spurred the development of techniques centered around its selection and optimization. However, this advancement

¹Our code, new datasets, and pre-trained model are available at <https://github.com/ExponentiAI/EffNet>.

has come at the cost of modeling complexity and a compromise in stability.

In this study, we experimentally discover that achieving favorable results can be accomplished with a simple methodology, while also enhancing the model’s generality to utilize any existing basic network as the backbone. Specifically, we simultaneously optimize feature distribution alignment intra- and inter-samples through structural design and loss function configuration. Illustrated in Fig. 1, (a) contrasts the traditional objective optimization method with our proposed approach (b). Our initial experiments revealed that single-branch encoders are susceptible to model training saturation issues. Therefore, we introduce a dual weight-sharing network structure to enhance the consistency of features within sketch and image samples, ensuring the model effectively learns key fine-grained features. Meanwhile, we replace the traditional triplet loss with the contrastive loss as the foundational loss function component for model target optimization, facilitating both intra-sample and inter-sample feature optimization concurrently. This strategic shift enables the model to accommodate more sample gradient information in each mini-batch, relieving limitations associated with the selection of positive and negative samples. Building upon this, we introduce a plug-and-play Token Representation Sharing Module (TRSM), further enhancing feature alignment in the joint embedding space and optimizing sample distribution through joint self-attention within samples and cross-attention between samples.

In summary, we introduce the EffNet, an efficient self-supervised FG-SBIR framework without complex methodology, the main contributions of this paper are as follows:

- We present the dual weight-sharing networks to enhance feature alignment within sketches and images, fostering distinctive feature representation within each modality. This also mitigates model learning saturation issues.
- We are the pioneers in proposing the utilization of self-supervised methods to concurrently optimize intra- and inter-sample feature distributions. This optimization also simplifies the data-loading approach.
- We design the TRSM, leveraging self-attention and cross-attention to facilitate information sharing between tokens, thereby further improving feature alignment intra- and inter-samples.
- Additionally, we introduce a new dataset named Clothes-V1, filling the gap in professional fashion clothing datasets in this field. Its multi-level quality can be valuable for other computer vision tasks as well.

Related Work

FG-SBIR

Fine-grained sketch-based image retrieval (FG-SBIR) involves retrieving images in a specific category based on a given sketch query. The evolution of FG-SBIR, from the introduction of triplet loss (Yu et al. 2016) to advancements in model learning capabilities through attention mechanisms (Song et al. 2017) and recent approaches like reinforcement learning (Muhammad et al. 2018; Bhunia et al. 2020, 2022a), meta-learning (Sain et al. 2021; Bhunia et al.

2022b), and sketch layered feature representation (Bhunia et al. 2020; Sain et al. 2020; Yang et al. 2021), has been rapid. However, these approaches rely on triplet loss and improve model performance by intricate methodologies. In contrast, our approach takes a different perspective by designing a simple and universal framework. This allows for easy replacement of the model backbone, yielding improved retrieval results without the need for complex design, data preprocessing, or parameter adjustments.

Contrastive Learning

Contrastive learning enhances similarity assessment among samples by maximizing positive sample similarity and minimizing negative sample similarity. In earlier work, (Wu et al. 2018) proposed the memory bank to store data features. Since then, (Ye et al. 2019) used data augmentation and changed the samples to come from each mini-batch. (Tian, Krishnan, and Isola 2020) learned a highly discriminative feature by taking images from multiple views as input. Similarly, (Chen et al. 2020) generated a large number of pos-neg sample pairs by using data augmentation and large batch size. To address the issue of sample selection bias during training, (He et al. 2020) proposed the momentum encoder. (Caron et al. 2020) used a clustering algorithm to reduce computational costs. These methods drive unsupervised representation learning to achieve superior performance, advancing downstream tasks in computer vision. Similarly, we can leverage the concept of contrastive learning to the field of FG-SBIR to enhance the encoder’s capacity for feature representation learning.

Vision Transformer

Vision Transformer (ViT) (Dosovitskiy et al. 2020) uses a self-attention mechanism, which provides a more effective way to model global image features compared to traditional CNN networks. Building upon ViT’s success, Han et al. (Han et al. 2021) proposed the TNT model by incorporating an additional Transformer network to capture the relationships between small patches in the patch sequence. In a similar vein, Liu et al. (Liu et al. 2021) introduced the Swin-ViT model, which utilizes a shift-window mechanism along with a multi-scale hierarchical structure to capture both local and global features. Due to the versatility and adaptability of the ViT model, it has been extended to methods in computer vision research that were previously limited to CNNs. However, only a few studies (Abhra et al. 2022; Sain et al. 2023) have explored ViT in the field of FG-SBIR. We believe that integrating ViT into FG-SBIR can further enhance retrieval performance. Therefore, we extend our proposed method to the ViT approaches in addition to the CNN methods.

How to Keep Learning?

We begin with an initial structure as shown in Fig. 2 (a), utilizing the prevalent pre-trained ViT-B/16 model (Dosovitskiy et al. 2020) as our backbone and modifying the dimensions of the classification layer to learn the representation of the inputs. However, we encountered a pivotal insight—the model’s performance exhibited saturation around the 150-epoch mark, and subsequent training iterations yielded neg-

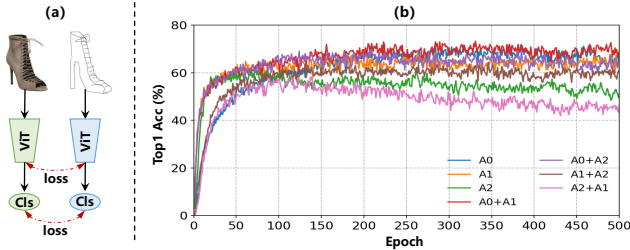


Figure 2: (a) A initial network for FG-SBIR. (b) Visualization of the training process. (A0: no augmentation. A1: added image scaling, rotation, and cropping operations. A2: similar to (He et al. 2020))

ligible enhancements, as illustrated by the A0 curve in Fig. 2 (b). We tried experimenting with conventional methodologies, such as data augmentation, output feature normalization, and increasing the number of classification layers. Regrettably, these methods did not show improvements. In terms of data augmentation, the intricate technique A2 appeared to drive the model into overfitting territory. On the other hand, the general data augmentation method scarcely induced any discernible benefit in the generalization capability of the model, as illustrated by the A1 curve in Fig. 2 (b).

Thus, arose the question of whether the model’s ability to learn better feature representations from input samples was impeded by its single-network architecture. Inspired by (Bromley et al. 1993), we surpass this limitation by replacing the original single network with dual weight-sharing networks. This change in approach enabled the model to optimize the feature distribution of both intra- and inter-samples, yielding more representative and discriminative feature representations. Furthermore, through an alternative preprocessing approach for inputs, we made a noteworthy observation: the inclusion of A0 within the processing method for the weight-sharing network consistently yielded superior outcomes compared to methods excluding A0. Intriguingly, the elaborate data augmentation strategy A2 proved to be incompatible with the nuances of fine-grained imagery, accentuating the risk of dampening the model’s generalization prowess and resulting in saturation. The A0+A1 curve in Fig. 2 (b) demonstrates the model’s enduring capacity to capture sample characteristics within the 500-epoch timeframe, and with an absence of pronounced feature degradation.

Methodology

Overview. In this study, we present an Effortless Self-Supervised Network for FG-SBIR (EffNet), as depicted in Fig. 3. It randomly selects pairs of sketch-image samples, amounting to the batch size. This elegantly streamlines the data-loading process compared to previous methods (Bhunia et al. 2022a; Sain et al. 2023). To counterbalance model saturation or even overfitting concerns, we introduce an architecture inspired by Siamese networks (Bromley et al. 1993). This innovation seamlessly integrates into both sketch and image encoders, facilitating feature distribution

alignment within sketch and image modalities. Additionally, we introduce a loss function based on contrastive learning method (Chen et al. 2020), facilitating self-supervised learning of the sketch and image encoder. This strategic incorporation further fosters feature distribution alignment within the sketches and images embedding space.

Feature Embedding

The emergence of Vision Transformer (ViT) (Chen et al. 2020) and its diverse iterations (Han et al. 2021; Liu et al. 2021; Zeng et al. 2022) has introduced a formidable alternative to the conventional Convolutional Neural Network (CNN) models (Simonyan and Zisserman 2014; He et al. 2016; Szegedy et al. 2016), profoundly enriching the landscape of downstream tasks within the realm of computer vision. Empowered by its remarkable prowess in feature extraction, we adopt the foundational ViT pre-training model, ViT-B/16-1K (Dosovitskiy et al. 2020), as the backbone for our sketch and image encoders, aptly denoted as \mathcal{E}_{skt} and \mathcal{E}_{img} .

As previously delineated, input samples are harnessed through our dataloader. Denoting the sketches and images within our dataset as \mathcal{S} and \mathcal{I} respectively, with the number of samples in each minibatch designated as m , we succinctly represent our data-loading process as $\mathcal{B}_m \Rightarrow \{s_j \in \mathcal{S}, i_j \in \mathcal{I} \mid s_j \text{ and } i_j \in \mathcal{R}^{224 \times 224 \times 3}\}$, and $j = 1, 2, \dots, m$. Initiating the feature extract process, we commence by applying data augmentation to the input samples \mathcal{B}_m , generating the sample pairs denoted as $\mathcal{B}'_m \Rightarrow \{(s_j, s'_j, i_j, i'_j) \mid s_j \in \mathcal{S}, i_j \in \mathcal{I}, s'_j \in \mathcal{S} \text{ and } i'_j \in \mathcal{I} \text{ are augmented samples}\}$. Subsequently, the augmented samples undergo patch encoding and positional encoding before respectively being fed into the encoders \mathcal{E}_{skt} and \mathcal{E}_{img} , obtaining the sketch features $\mathcal{F}_{skt} \Rightarrow \{f_{skt} \leftarrow \mathcal{E}_{skt}(s), f'_{skt} \leftarrow \mathcal{E}_{skt}(s')\}$ and image features $\mathcal{F}_{img} \Rightarrow \{f_{img} \leftarrow \mathcal{E}_{img}(i), f'_{img} \leftarrow \mathcal{E}_{img}(i')\}$ for the input samples \mathcal{B}_m . Notably, these features $f \in \mathcal{R}^{m \times 1 \times 768}$ are indicative of the feature representation located at the *class token*. Finally, the resulting features \mathcal{F}_{skt} and \mathcal{F}_{img} are channeled through a linear layer, mapping them into the $\mathcal{R}^{1 \times 512}$ dimension within the joint embedding space. This process yields the ultimate features \mathcal{F}_{skt}^{out} and \mathcal{F}_{img}^{out} for input sketch and image samples correspondingly.

Loss Function

Triplet Loss The conventional triplet loss (Bhunia et al. 2022a; Sain et al. 2023) mechanism involves the dataloader module loading anchor, positive, and negative samples for the model. The prevalent practice often entails selecting the sketch as the anchor and the image as positive and negative samples. Subsequently, these three samples are inputted into the model for feature extraction. The holistic optimization of the loss function is succinctly expressed as:

$$\mathcal{L}^{tri} = \max\{0, \|f_a - f_p\|^2 - \|f_a - f_n\|^2 + \alpha\} \quad (1)$$

where f_a , f_p , and f_n are the feature vectors of the anchor, positive and negative samples respectively, $\|\cdot\|$ is the norm of the vector (usually Euclidean distance), and α serves as the margin hyperparameter.

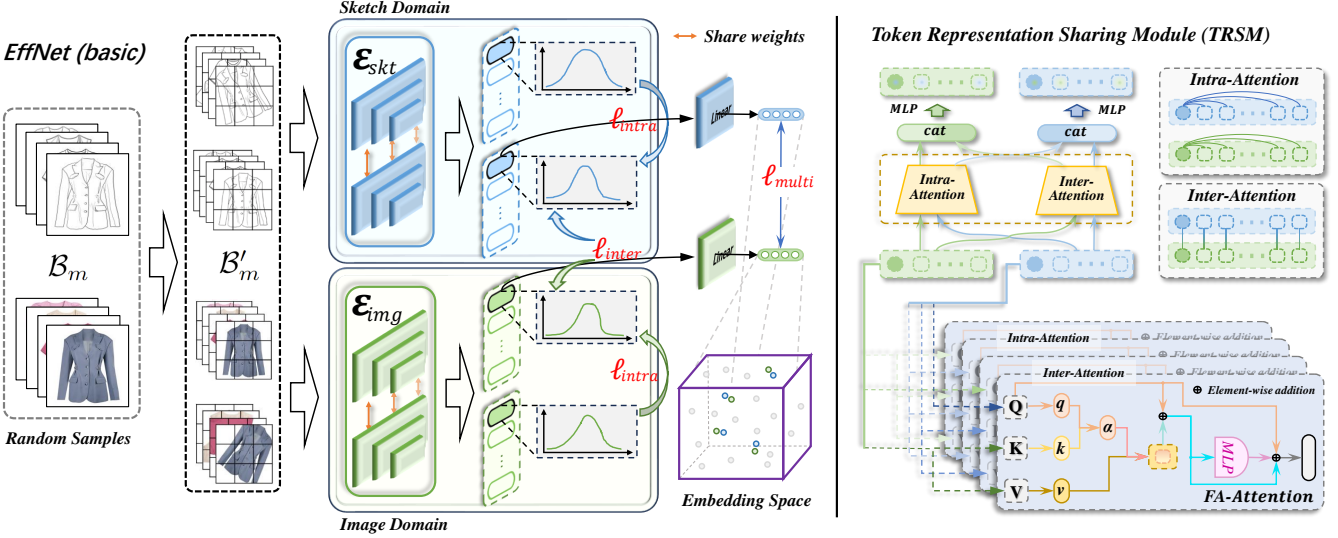


Figure 3: An overview of our EffNet framework (left). We adopt a randomized selection process to choose sketch-image sample pairs from the dataset. Subsequently, each mini-batch of sketches and images undergoes data augmentation before being fed into the ViT backbone network for feature encoding. Finally, the features associated with the *class token* within the sketch and image features, which have not undergone data enhancement, are seamlessly mapped to the embedding space through the utilization of a linear layer. Building upon this, we introduce the TRSM to further enhance feature alignment intra- and inter-samples via self-attention and cross-attention (right).

Contrastive Loss In our proposed framework, we introduce a loss function based on SimCLR (Chen et al. 2020), which can be expressed as follows:

$$\mathcal{L}(\mathcal{F}) = -\frac{1}{N} \sum_{i=1}^N \log \frac{\sum_{z=1}^{L-1} \exp((\mathcal{F}_i \cdot \mathcal{F}_{N.z+i}^\top)/\tau)}{\sum_{j=1}^L \mathbb{I}_{[i \neq j]} \exp((\mathcal{F}_i \cdot \mathcal{F}_j^\top)/\tau)} \quad (2)$$

Here, \mathcal{F} denotes an input feature vector derived from n sample vectors, and its construction follows $\mathcal{F} = \text{Cat}(\mathcal{F}_1, \mathcal{F}_2, \dots, \mathcal{F}_n)$, where Cat denotes the concatenation operation performed along the batch size dimension. N signifies the batch size, L represents the length of the concatenated feature vector, and τ serves as the temperature parameter. The indicator function $\mathbb{I}_{[i \neq j]} \in \{0, 1\}$ takes the value of 1 when $i \neq j$. Additionally, (\cdot) denotes the dot product operation applied to vectors, enabling the computation of the similarity matrix between two input samples.

Multi-Modal Loss. Our objective is to minimize the distance between the sketch and its corresponding image within the embedding space. We employ the fundamental loss function, referred to as multimodal loss, to fine-tune the distribution of encoded features obtained through the linear layers between sketches and images:

$$\ell_{multi} = \mathcal{L}(\mathcal{F}_{skt}^{out}, \mathcal{F}_{img}^{out}) \quad (3)$$

Intra-Sample Loss. To establish harmonious feature distribution alignment between the internal features of the sketch encoder \mathcal{E}_{skt} and the image encoder \mathcal{E}_{img} , we introduce the intra-sample loss ℓ_{intra} . It propels \mathcal{E}_{skt} and \mathcal{E}_{img} to learn the distinctive features inherent to the original images and their augmented counterparts in a self-supervised way, enhancing the capacity of feature representation:

$$\ell_{intra} = \mathcal{L}(f_{skt}, f'_{skt}) + \mathcal{L}(f_{img}, f'_{img}) \quad (4)$$

Inter-Sample Loss. Since the features of sketches and images obtained by \mathcal{E}_{skt} and \mathcal{E}_{img} should exhibit a high degree of similarity. We introduce an inter-sample loss that encourages a strong resemblance between these sketch features and image features, which aims to optimize their ultimate distribution within their joint embedding space:

$$\ell_{inter} = \mathcal{L}(f_{skt}, f_{img}) \quad (5)$$

In the final phase, the complete loss function of our framework is represented as follows:

$$\mathcal{L} = \ell_{multi} + \ell_{intra} + \ell_{inter} \quad (6)$$

Token Representation Sharing Module

As depicted on the right side of Fig. 3, we introduce the Token Representation Sharing Module (TRSM) to further enhance the feature alignment within and between sketch and image samples. TRSM comprises two primary components: Intra-Attention, facilitating feature interactions among tokens within a sample, and Inter-Attention, enabling interactions between tokens across samples. However, these components maintain separate sample representations. Hence, we merge the intra-sample and inter-sample interaction features, channeling them through a linear layer for the ultimate output. It's noted that TRSM is optional, as our basic EffNet (left part of Fig. 3) already yields commendable results.

During the model training phase, we first train the basic EffNet. Subsequently, we freeze the parameters in the EffNet model and insert TRSM, training its parameters for 200 epochs independently. Finally, we perform model inference on the overall trained model. Drawing inspiration from (Vaswani et al. 2017), we introduce FA-Attention as the core



Figure 4: Our newly proposed dataset, Clothes-V1, features sketches drawn by multiple designers with varying degrees of skill, giving it a professional and diverse character.

element of TRSM. FA-Attention computes attention scores between each token, thereby enriching the feature representation of the input sample, represented as:

$$\begin{aligned}
 \mathcal{F}_q &= Q \cdot W_q, \quad \mathcal{F}_k = K \cdot W_k, \quad \mathcal{F}_v = V \cdot W_v \\
 \text{Attn}(Q, K, V) &= \text{softmax}(\mathcal{F}_q \mathcal{F}_k^T / \sqrt{d_{\mathcal{F}_k}}) \mathcal{F}_v + \mathcal{F}_q \\
 \text{Linear}(X_1, X_2) &= \text{MLP}(X_2) + X_2 + X_1 \\
 \text{FA-Attention}(\mathcal{F}_1, \mathcal{F}_2) &= \text{Linear}(\mathcal{F}_1, \text{Attn}(\mathcal{F}_1, \mathcal{F}_2, \mathcal{F}_2))
 \end{aligned} \tag{7}$$

where W_q , W_k , and W_v are responsible for mapping input token embeddings into queries, keys, and values.

In this way, our approach can facilitate the model to simultaneously focus on intra-modal and inter-modal information through both self-attention and cross-attention, thereby further enhancing the overall retrieval performance.

Experiments

Experimental Settings

Clothes-V1. Existing fine-grained sketch-based image retrieval (FG-SBIR) datasets (Yu et al. 2016) present several challenges: (i) There is a limited number of images without corresponding sketches. (ii) The sketches are drawn in a single rough style. (iii) Fashion clothing, being an essential aspect of our daily lives and a topic of interest for many individuals, lacks a dedicated dataset in the FG-SBIR field for fashion designers. To address these limitations, we invited four professional designers (over five years) and three junior designers (over one year or design novice). This diverse team composition ensures a wide range of sketch styles and levels of expertise, making the dataset more representative of real-life scenarios. **Its specialized nature and diverse collection** of fashion sketches make it a valuable resource for various tasks, including FG-SBIR, image generation, image translation, and fashion-related research.

Specifically, Clothes-V1 has 1200 (500) sketches (images), containing 925 (380) and 275 (120) for the training and validation set. Each image corresponds to at least 1 sketch and at most 5 sketches. The dataset is further categorized into types, such as sweaters, shirts, jackets, dresses, cheongsams, etc. Moreover, we are actively working to continuously expand our dataset as soon as possible.

Datasets. We use two publicly available datasets *QMUL-Chair-V2* and *QMUL-Shoe-V2* (Yu et al. 2016) along with our self-collected dataset Clothes-V1 to evaluate the performance of our proposed framework. The *QMUL-Chair-V2* includes 964 (300) and 311 (100) sketches (images) for the training set and validation set, and the *QMUL-Chair-V2* includes 5982 (1800) and 666 (200) sketches (images) for the training set and validation set.

Implementation Details. Our model is implemented using the PyTorch framework and is based on the ViT-B/16-1K model (Dosovitskiy et al. 2020). The input size is 224×224 , the final embedding vector's dimension is 512, and the temperature parameter τ is 0.07. We train the model on a single NVIDIA 32GB Tesla V100 GPU, using a batch size of 16 and the Adam optimizer (Kingma and Ba 2014) with a learning rate of 6e-6 and weight decay of 1e-4, and the training process lasts for 500 epochs. In addition, we incorporated other pre-trained models VGG16 (Simonyan and Zisserman 2014), ResNet50 (He et al. 2016), InceptionV3 (Szegedy et al. 2016), and Swin-ViT (Liu et al. 2021) to further verify the adaptability and efficacy of our framework.

Evaluation Metrics. We utilize the widely used Acc.@1, Acc.@5, and Acc.@10 to quantify the retrieval performance, which represents the probability of the correct image appearing in the first 1, 5, and 10 retrieved results, respectively.

Competitors

We compared our approach against 12 state-of-the-art methods: **Triplet-SN** (Yu et al. 2016) adopts triplet loss for model training. **Triplet-Att-SN** (Song et al. 2017) introduces an attention module to improve detailed features. **On-TheFly** (Bhunia et al. 2020) employs reinforcement learning and multi-stage sketch input to retrieve more quickly. **B-Siamese** (Sain et al. 2020) is builds on *Triplet-SN*, but with a stronger backbone. **CMHM-SBIR** (Sain et al. 2020) proposes a co-attention module to model cross-modal multi-level structures. **SketchAA** (Yang et al. 2021) proposes a multi-granularity modeling approach for representing sketch appearance and structural features. **Semi-Sup** (Bhunia et al. 2021) introduces a semi-supervised framework for cross-modal retrieval. **StyleMeUp** (Sain et al. 2021) proposes a meta-learning framework for generalizing to unseen sketch styles. **Adpt-SBIR** (Bhunia et al. 2022b) introduces a model-agnostic meta-learning framework. **Part-SBIR** (Chowdhury et al. 2022) proposes cross-modal domain associations in a part-aware manner using optimal transport. **NT-SBIR** (Bhunia et al. 2022a) proposes a framework for sketch stroke subset selection based on reinforcement learning. **EUPS-SBIR** (Sain et al. 2023) proposes using a triplet loss within a modality and pre-training a teacher model on a large set of unlabeled photos.

Results

Performance Analysis

FG-SBIR. As presented in Table 1, our proposed model exhibits superior performance compared to the baselines. Notably, our model achieves new state-of-the-art results

Table 1: Comparative results of our model against other methods on QMUL-Chair-V2, QMUL-Shoe-V2, and Clothes-V1.

Methods	Venue	QMUL-Chair-V2(%)			QMUL-Shoe-V2(%)			Clothes-V1(%)		
		Acc.@1	Acc.@5	Acc.@10	Acc.@1	Acc.@5	Acc.@10	Acc.@1	Acc.@5	Acc.@10
Triplet-SN	CVPR'16	33.75	65.94	79.26	18.62	43.09	59.31	64.36	85.82	92.73
Triplet-Att-SN	ICCV'17	37.15	67.80	82.97	22.67	51.20	65.02	70.18	83.64	91.64
B-Siamese	BMVC'20	40.56	71.83	85.76	20.12	48.95	63.81	84.73	97.82	99.27
CMHM-SBIR	BMVC'20	51.70	80.50	88.85	29.28	59.76	74.62	-	-	-
OnTheFly	CVPR'20	39.01	75.85	87.00	35.91	66.78	78.54	63.27	90.18	92.73
SketchAA	ICCV'21	52.89	-	94.88	32.22	-	79.63	-	-	-
Semi-Sup	CVPR'21	60.20	78.10	90.81	39.10	69.90	87.50	-	-	-
StyleMeUp	CVPR'21	62.86	79.60	91.14	36.47	68.10	81.83	-	-	-
Adpt-SBIR	ECCV'22	-	-	-	38.30	76.60	-	-	-	-
Part-SBIR	CVPR'22	63.30	79.70	-	39.90	68.20	82.90	-	-	-
NT-SBIR	CVPR'22	64.80	79.10	-	43.70	74.90	-	-	-	-
EUPS-SBIR	CVPR'23	71.22	-	92.18	44.18	-	84.68	-	-	-
EffNet	Ours	73.31	93.24	97.15	40.11	67.54	79.29	94.12	98.91	99.27
EffNet+TRSM	Ours	74.28	93.89	97.43	39.94	71.47	82.88	94.91	98.91	98.91



Figure 5: Qualitative comparison results between our method (blue) and Triplet-Att-SN (green) on QMUL-Chair-V2.

on the *QMUL-Chair-V2* and *Clothes-V1*, while also delivering good results on the *QMUL-Shoe-V2*. Previous approaches (Yu et al. 2016; Song et al. 2017) exhibited poor performance due to the underperformance of the Sketch-A-Net backbone network (Yu et al. 2017). Subsequent studies have replaced it with a stronger backbone (Sain et al. 2020), while considering the problem from different perspectives of sketches and images, and utilizing reinforcement learning (Bhunia et al. 2020, 2022a), meta-learning (Sain et al. 2021; Bhunia et al. 2022b), and other technologies (Yang et al. 2021; Bhunia et al. 2021; Chowdhury et al. 2022; Sain et al. 2023) to continuously improve retrieval performance. (i) **QMUL-Chair-V2**: Our model’s Top5 accuracy surpasses EUPS-SBIR’s Top10 accuracy, and for NT-SBIR, ours outperforms nearly 10% on Top1 accuracy. (ii) **QMUL-Shoe-V2**: While our model didn’t secure the top rank, it still demonstrates encouraging potential, boasting a slight disparity of approximately 4% in Top1 accuracy compared to

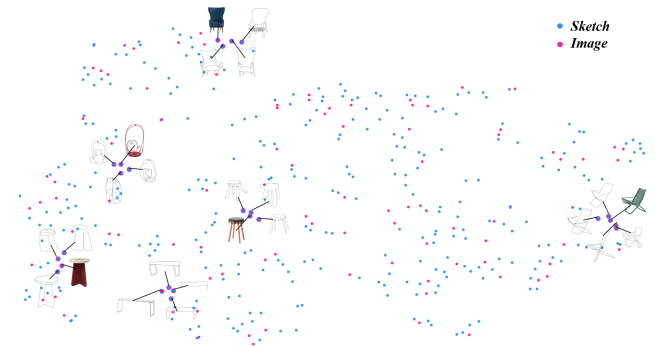


Figure 6: t-SNE visualizations of sketch feature (blue) and image feature (pink) embeddings in a joint embedding space on QMUL-Chair-V2 (Zoom in for better visualization).

EUPS-SBIR. Remarkably, our model clinches the third position among competing SOTA approaches. The performance gap of our model can be attributed to the dataset’s larger size and the relatively lower specificity of shoe sketches compared to the chair and clothes. This disparity culminates in a phenomenon where the samples become more closely clustered within the acquired embedding space. (iii) **Clothes-V1**: The results demonstrate a clear advantage of our model in Top1 and Top5 accuracy, along with an impressive nearly 100% accuracy in Top10. These outcomes underscore our model’s remarkable retrieval capabilities when confronted with multi-level style variations in sketches. In general, we approach the network structure from a different perspective, aiming to achieve better results in the simplest manner possible, without the need for complex and cumbersome designs compared to other methods. Based on the basic EffNet, our TRSM can further enhance the model’s feature representation capacity for input samples, considering both intra-sample and inter-sample perspectives. The experimental results demonstrate the excellent performance of our method.

Retrieval Performance. We present the Top 5 comparative

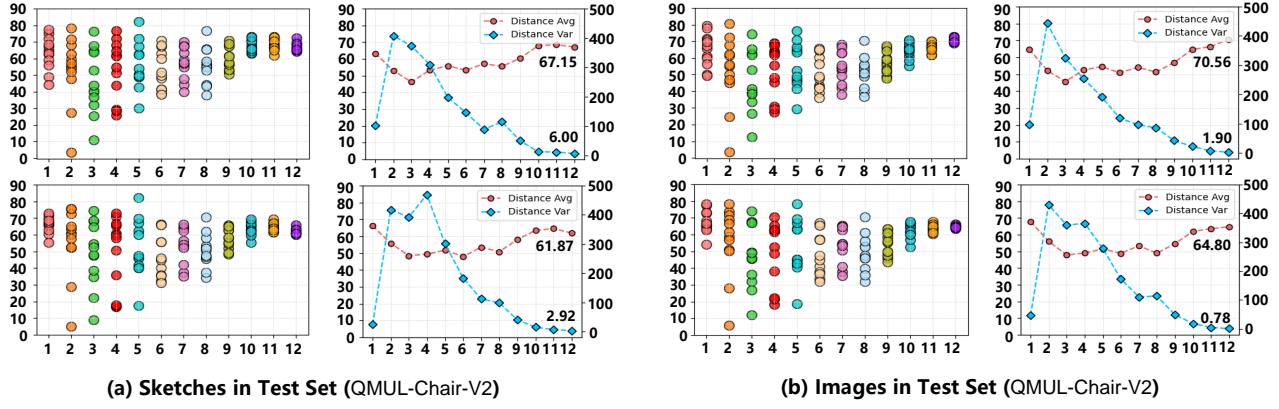


Figure 7: The average attention distance in multi-heads (dots) w.r.t the layers on the pre-trained ViT model (above) and our trained model (below).

retrieval performance and the Top 10 retrieval results of our methods in Fig. 5. It is evident that the corresponding images retrieved by our method achieve better ranking results in Acc. @ 5 (top). The top-retrieved image in the Acc. @ 10 also exhibits a significant similarity to the provided sketch (bottom). Furthermore, in the second row, all the top ten results feature chairs with backrests. Despite the ground truth being the second image, the first one bears a striking resemblance to the provided sketch from a human visual perspective. These highlight our stronger retrieval performance.

Feature Embedding. To visualize the distribution of encoded sketch and image feature vectors in the joint embedding space, we utilize the t-SNE (Van der Maaten and Hinton 2008) dimensionality reduction algorithm to map them to a two-dimensional representation. The resulting visualization, depicted in Fig. 6, illustrates a relatively even distribution of features across the two modalities. It demonstrates a close distribution between images and their corresponding sketches, irrespective of the number of sketches associated with each image. This indicates the success of our method in extracting and encoding shared key information from both sketches and images, effectively optimizing sample feature distribution within the joint embedding space and consequently yielding better retrieval results.

Attention Distance. As illustrated in Fig. 7, we compute the average attention distance of multi-heads attention for each layer within the ViT model, along with the mean and variance of attention distance for each layer. A reduced mean signifies a model preference for local features, while a diminished variance indicates consistent attention-head distances, yielding more stable features. Extensive experimental results reveal that our method guides the ViT model to concentrate on finer details and heighten feature similarity. This aligns with the demands of fine-grained images and underscores the framework’s feature alignment effect.

Ablation Study

To evaluate the effectiveness of our proposed method, we conducted ablation studies on QMUL-Chair-V2 (Yu et al. 2016) as a representative.

Framework. The experimental results in Table 2 represent

Table 2: Ablation Studies on our framework ((i) Double: the use of our dual weight-sharing networks. (ii) Single: no utilization).

ID	Methods	Backbone	ℓ_{inter}	QMUL-Chair-V2(%)		
				Acc. @ 1	Acc. @ 5	Acc. @ 10
1	Single	VGG16	✗	22.42	56.23	74.38
2	Single	InceptionV3	✗	39.86	78.29	90.04
3	Single	ResNet50	✗	36.66	74.73	86.48
4	Single	ViT-B/16	✗	59.43	89.32	95.02
5	Single	Swin-ViT	✗	62.63	93.24	97.51
6	Double	VGG16	✗	31.32	64.77	81.14
7	Double	InceptionV3	✗	42.71	80.43	90.39
8	Double	ResNet50	✗	42.35	72.95	85.41
9	Double	ViT-B/16	✗	58.36	90.75	95.37
10	Double	Swin-ViT	✗	63.35	90.75	95.37
11	Double	VGG16	✓	46.26	79.00	86.83
12	Double	InceptionV3	✓	46.26	82.56	91.82
13	Double	ResNet50	✓	48.04	81.14	89.32
14	Double	ViT-B/16	✓	73.31	93.24	97.15
15	Double	Swin-ViT	✓	73.31	93.95	98.22

that our dual weight-sharing networks can significantly enhance the overall performance of the model across various mainstream backbone networks. Particularly, the improvement effect is more evident when applied to the ViT-based models. The improved model performance is attributed to the discriminative power of our framework, enabling better representation between similar and dissimilar samples within complex data distributions. In essence, our framework takes into account both the single feature distribution within the sketches and images while considering the joint feature distribution of the sketches and images, resulting in more representative feature representations. As a result, the model achieves enhanced performance in distinguishing diverse samples and improving overall accuracy. Furthermore, our observations revealed that the inclusion of ℓ_{inter} not only elevates the overall model performance but also expedites the convergence trajectory. This can be attributed to its ability to further enhance the feature alignment between sketches and images based on the dual weight-sharing networks’ improved feature alignment within sketches and im-

Table 3: Quantitative results of different ways to load datasets ((i) Augment: A0 with no augmentation. A1 adds image scaling, rotation, and cropping operations. A2 is similar to (He et al. 2020). (ii) Loss: C represents the Contrastive loss and T represents the Triplet loss).

ID	Methods	Augment	Loss	QMUL-Chair-V2(%)		
				Acc.@1	Acc.@5	Acc.@10
1	Single	A0	C	59.43	89.32	95.02
2	Single	A1	C	68.33	90.39	95.73
3	Single	A2	C	61.92	91.04	96.44
4	Double	A0+A1	C	73.31	93.24	97.15
5	Double	A0+A2	C	69.75	92.17	95.37
6	Double	A1+A2	C	64.41	87.19	93.24
7	Double	A2+A1	C	58.36	85.41	91.82
8	sketch (anchor)	A0	T	57.65	89.83	96.09
9	sketch (anchor)	A1	T	55.52	87.90	95.37
10	sketch (anchor)	A2	T	51.60	81.85	90.75
11	image (anchor)	A0	T	24.20	51.96	68.68
12	image (anchor)	A1	T	16.01	41.64	55.87
13	image (anchor)	A2	T	17.44	41.28	58.36

ages. This augmented alignment contributes to the extraction of more distinctive and representative features by the dual weight-sharing networks.

Dataloader. As depicted in Table 3, we use three different data processing strategies to compare two data-loading methods based on the contrastive loss function (CLF) and based on the triplet loss function (TLF). We categorize the previous TLF-based methods into two groups: (i) uses the image as the anchor and selects the sketch as positive and negative samples, and (ii) uses the sketch as the anchor and selects the image as positive and negative samples. It is evident that the TLF-based methods perform lower than the CLF-based methods without any other optimization. This is due to our loss function optimizing the model comprehensively intra- and inter-samples, with the contrastive loss providing greater gradient contrast information in each mini-batch update, leading to an improvement in the overall performance. Moreover, it also eliminates the need for selecting positive and negative samples, reducing the burden of sample selection.

Further Discussion on Modality Fusion

Cross-ViT. As cross-attention holds significance in cross-modal tasks, we integrated the Cross-ViT module (Chen, Fan, and Panda 2021) into our basic EffNet to evaluate its impact on the FG-SBIR task. The structure principle is illustrated in Fig 8, we discussed two situations: one (i) involves directly replacing the *class token* and the other (ii) entails directly splicing the *class token*, for the *Cross Block* on the right is the principle of the cross-attention module. As depicted in Table 4, we conducted experiments in three aspects: the number of layers η of the *Cross Block*, the number of attention heads in the *Cross Block*, and the different modality fusion methods. It’s noticeable that incorporating the cross-attention module results in a minor decline in model performance, with fluctuations remaining relatively stable. Despite a slight enhancement in specific metrics, the overall improvement is not substantial. This can

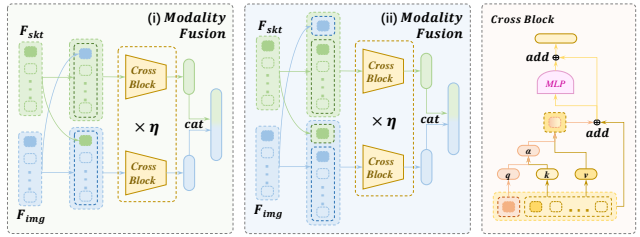


Figure 8: An overview of different Modality Fusion methods.

Table 4: Quantitative results of the cross-attention in Modality Fusion.

ID	Fusion Methods	Layers (η)	Num heads	QMUL-Chair-V2(%)		
				Acc.@1	Acc.@5	Acc.@10
1	i	5	12	70.11	91.82	96.09
2	i	3	12	72.95	92.88	96.09
3	i	1	12	71.53	92.88	96.09
4	i	3	6	72.24	93.95	96.44
5	i	3	24	71.89	92.88	96.44
6	i	3	1	70.46	93.24	96.09
7	ii	3	12	71.53	92.53	96.80
Ours	-	-	-	73.31	93.24	97.15

be attributed to the fact that the input features already possess high semantic information and expressive power, making it challenging for the cross-attention module to further optimize their representation. Moreover, the introduction of the cross-attention module requires the sketch and image encoders to learn to project features into a shared embedding space, which may lead to the loss of some discriminative features and, consequently, a slight increase in the error between paired objects. Additionally, keeping the number of attention heads constant and excessively increasing the number of cross-attention module layers results in a significant performance drop, further supporting our observations. These results indicate that solely considering modal mixing has less impact on the FG-SBIR task, thereby validating the effectiveness of our TRSM. More visualization of the research results can be found on our GitHub.

Conclusion

In this paper, we present EffNet, a novel FG-SBIR solution, along with a versatile professional clothing dataset, Cloth-V1. Our approach incorporates structural and loss function design, enabling the model to concurrently focus on intra-sample and inter-sample feature alignment, thereby optimizing the sample distribution within the joint embedding space to improve retrieval performance. Our proposed method exhibits strong scalability, accommodating various mainstream backbones as feature extraction networks, and offers straightforward implementation. Furthermore, we introduce TRSM to further refine sample feature distribution based on self-attention and cross-attention mechanisms among tokens. Extensive experiments demonstrate that our EffNet achieves superior retrieval performance across several benchmarks.

References

Abhra et al. 2022. Cross-Modal Fusion Distillation for Fine-Grained Sketch-Based Image Retrieval. In *BMVC*.

Baldrati, A.; Morelli, D.; Cartella, G.; Cornia, M.; Bertini, M.; and Cucchiara, R. 2023. Multimodal garment designer: Human-centric latent diffusion models for fashion image editing. In *Proceedings of the IEEE/CVF International Conference on Computer Vision*, 23393–23402.

Bhunia, A. K.; Chowdhury, P. N.; Sain, A.; Yang, Y.; Xiang, T.; and Song, Y.-Z. 2021. More photos are all you need: Semi-supervised learning for fine-grained sketch based image retrieval. In *Proceedings of the IEEE/CVF conference on Computer Vision and Pattern Recognition*, 4247–4256.

Bhunia, A. K.; Koley, S.; Khilji, A. F. U. R.; Sain, A.; Chowdhury, P. N.; Xiang, T.; and Song, Y.-Z. 2022a. Sketching without worrying: Noise-tolerant sketch-based image retrieval. In *Proceedings of the IEEE/CVF Conference on Computer Vision and Pattern Recognition*, 999–1008.

Bhunia, A. K.; Sain, A.; Shah, P. H.; Gupta, A.; Chowdhury, P. N.; Xiang, T.; and Song, Y.-Z. 2022b. Adaptive fine-grained sketch-based image retrieval. In *European Conference on Computer Vision*, 163–181. Springer.

Bhunia, A. K.; Yang, Y.; Hospedales, T. M.; Xiang, T.; and Song, Y.-Z. 2020. Sketch less for more: On-the-fly fine-grained sketch-based image retrieval. In *Proceedings of the IEEE/CVF Conference on Computer Vision and Pattern Recognition*, 9779–9788.

Bromley, J.; Guyon, I.; LeCun, Y.; Säckinger, E.; and Shah, R. 1993. Signature verification using a “siamese” time delay neural network. *Advances in neural information processing systems*, 6.

Caron, M.; Misra, I.; Mairal, J.; Goyal, P.; Bojanowski, P.; and Joulin, A. 2020. Unsupervised learning of visual features by contrasting cluster assignments. *Advances in neural information processing systems*, 33: 9912–9924.

Chen, C.-F.; Fan, Q.; and Panda, R. 2021. CrossViT: Cross-Attention Multi-Scale Vision Transformer for Image Classification. *arXiv:2103.14899*.

Chen, T.; Kornblith, S.; Norouzi, M.; and Hinton, G. 2020. A simple framework for contrastive learning of visual representations. In *International conference on machine learning*, 1597–1607. PMLR.

Chowdhury, P. N.; Bhunia, A. K.; Gajjala, V. R.; Sain, A.; Xiang, T.; and Song, Y.-Z. 2022. Partially does it: Towards scene-level fg-sbir with partial input. In *Proceedings of the IEEE/CVF Conference on Computer Vision and Pattern Recognition*, 2395–2405.

Deng, H.; Jiang, J.; Yu, Z.; Ouyang, J.; and Wu, D. 2024. CrossGAI: A Cross-Device Generative AI Framework for Collaborative Fashion Design. *Proceedings of the ACM on Interactive, Mobile, Wearable and Ubiquitous Technologies*, 8(1): 1–27.

Dosovitskiy, A.; Beyer, L.; Kolesnikov, A.; Weissenborn, D.; Zhai, X.; Unterthiner, T.; Dehghani, M.; Minderer, M.; Heigold, G.; Gelly, S.; et al. 2020. An image is worth 16x16 words: Transformers for image recognition at scale. *arXiv preprint arXiv:2010.11929*.

Han, K.; Xiao, A.; Wu, E.; Guo, J.; Xu, C.; and Wang, Y. 2021. Transformer in transformer. In *NeurIPS*.

He, K.; Fan, H.; Wu, Y.; Xie, S.; and Girshick, R. 2020. Momentum contrast for unsupervised visual representation learning. In *Proceedings of the IEEE/CVF conference on computer vision and pattern recognition*, 9729–9738.

He, K.; Zhang, X.; Ren, S.; and Sun, J. 2016. Deep residual learning for image recognition. In *Proceedings of the IEEE conference on computer vision and pattern recognition*, 770–778.

Kingma, D. P.; and Ba, J. 2014. Adam: A method for stochastic optimization. *arXiv preprint arXiv:1412.6980*.

Liu, Z.; Lin, Y.; Cao, Y.; Hu, H.; Wei, Y.; Zhang, Z.; Lin, S.; and Guo, B. 2021. Swin Transformer: Hierarchical Vision Transformer using Shifted Windows. In *Proceedings of the IEEE/CVF International Conference on Computer Vision (ICCV)*.

Muhammad, U. R.; Yang, Y.; Song, Y.-Z.; Xiang, T.; and Hospedales, T. M. 2018. Learning deep sketch abstraction. In *Proceedings of the IEEE Conference on Computer Vision and Pattern Recognition*, 8014–8023.

Pang, K.; Yang, Y.; Hospedales, T. M.; Xiang, T.; and Song, Y.-Z. 2020. Solving mixed-modal jigsaw puzzle for fine-grained sketch-based image retrieval. In *Proceedings of the IEEE/CVF Conference on Computer Vision and Pattern Recognition*, 10347–10355.

Sain, A.; Bhunia, A. K.; Koley, S.; Chowdhury, P. N.; Chattopadhyay, S.; Xiang, T.; and Song, Y.-Z. 2023. Exploiting Unlabelled Photos for Stronger Fine-Grained SBIR. In *Proceedings of the IEEE/CVF Conference on Computer Vision and Pattern Recognition*, 6873–6883.

Sain, A.; Bhunia, A. K.; Yang, Y.; Xiang, T.; and Song, Y.-Z. 2020. Cross-modal hierarchical modelling for fine-grained sketch based image retrieval. *arXiv preprint arXiv:2007.15103*.

Sain, A.; Bhunia, A. K.; Yang, Y.; Xiang, T.; and Song, Y.-Z. 2021. Stylemeup: Towards style-agnostic sketch-based image retrieval. In *Proceedings of the IEEE/CVF conference on computer vision and pattern recognition*, 8504–8513.

Simonyan, K.; and Zisserman, A. 2014. Very deep convolutional networks for large-scale image recognition. *arXiv preprint arXiv:1409.1556*.

Song, J.; Yu, Q.; Song, Y.-Z.; Xiang, T.; and Hospedales, T. M. 2017. Deep spatial-semantic attention for fine-grained sketch-based image retrieval. In *Proceedings of the IEEE international conference on computer vision*, 5551–5560.

Szegedy, C.; Vanhoucke, V.; Ioffe, S.; Shlens, J.; and Wojna, Z. 2016. Rethinking the inception architecture for computer vision. In *Proceedings of the IEEE conference on computer vision and pattern recognition*, 2818–2826.

Tian, Y.; Krishnan, D.; and Isola, P. 2020. Contrastive multiview coding. In *Computer Vision–ECCV 2020: 16th European Conference, Glasgow, UK, August 23–28, 2020, Proceedings, Part XI 16*, 776–794. Springer.

Van der Maaten, L.; and Hinton, G. 2008. Visualizing data using t-SNE. *Journal of machine learning research*, 9(11).

Vaswani, A.; Shazeer, N.; Parmar, N.; Uszkoreit, J.; Jones, L.; Gomez, A. N.; Kaiser, Ł.; and Polosukhin, I. 2017. Attention is all you need. *Advances in neural information processing systems*, 30.

Wang, H.; Fu, T.; Du, Y.; Gao, W.; Huang, K.; Liu, Z.; Chandak, P.; Liu, S.; Van Katwyk, P.; Deac, A.; et al. 2023. Scientific discovery in the age of artificial intelligence. *Nature*, 620(7972): 47–60.

Wang, L.; Qian, X.; Zhang, Y.; Shen, J.; and Cao, X. 2019. Enhancing sketch-based image retrieval by cnn semantic re-ranking. *IEEE transactions on cybernetics*, 50(7): 3330–3342.

Wei, X.-S.; Song, Y.-Z.; Mac Aodha, O.; Wu, J.; Peng, Y.; Tang, J.; Yang, J.; and Belongie, S. 2021. Fine-grained image analysis with deep learning: A survey. *IEEE transactions on pattern analysis and machine intelligence*, 44(12): 8927–8948.

Wu, D.; Yu, Z.; Ma, N.; Jiang, J.; Wang, Y.; Zhou, G.; Deng, H.; and Li, Y. 2023. StyleMe: Towards Intelligent Fashion Generation with Designer Style. In *Proceedings of the 2023 CHI Conference on Human Factors in Computing Systems*, 1–16.

Wu, Z.; Xiong, Y.; Stella, X. Y.; and Lin, D. 2018. Unsupervised Feature Learning via Non-Parametric Instance Discrimination. In *Proceedings of the IEEE Conference on Computer Vision and Pattern Recognition*.

Xu, J.; Liu, X.; Wu, Y.; Tong, Y.; Li, Q.; Ding, M.; Tang, J.; and Dong, Y. 2024. Imagereward: Learning and evaluating human preferences for text-to-image generation. *Advances in Neural Information Processing Systems*, 36.

Xu, P.; Hospedales, T. M.; Yin, Q.; Song, Y.-Z.; Xiang, T.; and Wang, L. 2022. Deep learning for free-hand sketch: A survey. *IEEE transactions on pattern analysis and machine intelligence*, 45(1): 285–312.

Yang, L.; Pang, K.; Zhang, H.; and Song, Y.-Z. 2021. Sketchaa: Abstract representation for abstract sketches. In *Proceedings of the IEEE/CVF International Conference on Computer Vision*, 10097–10106.

Ye, M.; Zhang, X.; Yuen, P. C.; and Chang, S.-F. 2019. Unsupervised Embedding Learning via Invariant and Spreading Instance Feature. In *IEEE International Conference on Computer Vision and Pattern Recognition (CVPR)*.

Yu, Q.; Liu, F.; Song, Y.-Z.; Xiang, T.; Hospedales, T. M.; and Loy, C.-C. 2016. Sketch me that shoe. In *Proceedings of the IEEE Conference on Computer Vision and Pattern Recognition*, 799–807.

Yu, Q.; Song, J.; Song, Y.-Z.; Xiang, T.; and Hospedales, T. M. 2021. Fine-grained instance-level sketch-based image retrieval. *International Journal of Computer Vision*, 129(2): 484–500.

Yu, Q.; Yang, Y.; Liu, F.; Song, Y.-Z.; Xiang, T.; and Hospedales, T. M. 2017. Sketch-a-net: A deep neural network that beats humans. *International Journal of Computer Vision*, 122(3): 411–425.

Zeng, W.; Jin, S.; Liu, W.; Qian, C.; Luo, P.; Ouyang, W.; and Wang, X. 2022. Not all tokens are equal: Human-centric visual analysis via token clustering transformer. In *Proceedings of the IEEE/CVF Conference on Computer Vision and Pattern Recognition*, 11101–11111.